IEEE Access
Multidisciplinary | Rapid Review | Open Access Journal

Received 20 June 2023, accepted 2 August 2023, date of publication 7 August 2023, date of current version 15 August 2023.

Digital Object Identifier 10.1109/ACCESS.2023.3303207

RESEARCH ARTICLE

High-Frequency Planar Transformer Based on Interleaved Serpentine Winding Method With Low Parasitic Capacitance for High-Current Input LLC Resonant Converter

SU-SEONG PARK, MYEONG-SEOK JEON, SUNG-SOO MIN, AND RAE-YOUNG KIM, (Senior Member, IEEE)

Department of Electrical and Biomedical Engineering, Hanyang University, Seoul 04763, South Korea

Corresponding author: Rae-Young Kim (rykim@hanyang.ac.kr)

This work was supported by the Korea Institute of Energy Technology Evaluation and Planning (KETEP) grant funded by the Korean Government Ministry of Trade, Industry and Energy (Development of High Efficiency Power Converter based on Multidisciplinary Design and Optimization Platform) under Grant 2018201010650A and Grant 20212020800020.

ABSTRACT An LLC resonant converter should have high efficiency and power density. Further, it is important to reduce the volume and loss of the transformer, which provides insulation and voltage conversion between the input and output. When a planar core is used to achieve high power density, the magnitude of the parasitic components and the transformer loss considerably depend on the winding arrangement within the limited window area. Therefore, analyzing the various winding arrangements is necessary. To this end, an interleaved serpentine winding method that reduces the winding loss attributed to the high current by maximizing the window area of the planar core is proposed. It has advantages of low parasitic capacitance and excellent assembly is proposed for this method. The proposed winding method uses a Litz wire to reduce the DC copper loss, and it does not require additional space for the winding arrangement compared to that required by the U-type winding method. The capacitive energy distribution of the proposed winding method is compared with that of the existing U-type winding method to confirm the parasitic capacitance reduction effect of the proposed winding method. The formulae for calculating the effective capacitance of each winding method are derived for accurately estimating the parasitic capacitance. Finally, the effectiveness of the proposed analysis method and prototype are verified through finite element analysis simulation and experiments and it shows improvement of LLC Converter operation and the overall efficiency increases about 0.5%.

INDEX TERMS LLC resonant converter, planar transformer, serpentine winding method, interleaving winding, low parasitic capacitance, high efficiency, high power density, high frequency.

I. INTRODUCTION

Among the many DC–DC converter topologies, the LLC resonant converter can achieve high efficiency using soft switching, and it also exhibits excellent output voltage control characteristics under light load conditions [1]. In addition, the stable operation of the converter is guaranteed because the primary and secondary sides are isolated by the transformer. Given these advantages, the LLC resonant converters have various applications, such as in electric vehicle chargers, solar power converters, and fuel cell converters [2], [3]. The LLC resonant converter includes several components such as Cap, Inductor, Transformer. The high-frequency transformer plays an important role in ensuring the isolation and voltage conversion between the input and output. The high-frequency transformer occupies a relatively large volume in the overall LLC resonant converter PCB, and therefore, the overall size of the converter can be reduced when a

The associate editor coordinating the review of this manuscript and approving it for publication was Zhong Wu.

low-profile core is used, which also leads to an improvement in power density. The Litz wire and PCB pattern can be used as windings in a flat transformer that uses a low-profile core [4], [5]. However, a large parasitic capacitance between the layers needs to be considered when using the PCB winding method. Therefore, various studies on the effective arrangement of PCB patterns and vias have been conducted when using the PCB winding method [6], [7], [8], [9]. In [6] and [7], a winding arrangement that minimizes the overlapping area between the PCB layers to reduce parasitic capacitance was proposed. In [8] and [9], arrangements that reduces potential differences between the PCB patterns and layers were presented; a method for minimizing the capacitive energy stored in the parasitic capacitance was also proposed.

Studies have also focused on winding structures that can reduce AC losses using the PCB winding method [10], [11], [12], [13]. These studies reduce the AC loss attributed to the proximity effect by offsetting the electromotive force in each layer through an interleaving arrangement. This arrangement alternately crosses the primary and secondary winding PCBs. Even though using multiple interleaving layers, increasing the current capacity is difficult because the conductor cross-sectional area is limited by the insulation layer in the PCB. Even if many PCBs are used to handle high currents, their high manufacturing costs can be a problem [4].

In contrast, wire winding using a Litz wire, which is composed of a bunch of thin copper wires coated with insulating materials, such as enamel and nylon, can easily secure the cross-sectional area of the conductor compared to that using the PCB winding method. Therefore, it can also increase the current capacity. Further, the losses caused by the skin and proximity effects of the conductor are small, and the manufacturing cost is lower than that of the PCB winding method. Therefore, a Litz wire should be used instead of a PCB pattern when the converter operates under high-current operating conditions. However, the Litz wire generates parasitic capacitance when a planar core is applied to increase the power density under high-current operating conditions. Thus, a method for effectively decreasing the space between each winding should be developed.

An optimal winding arrangement method that can reduce parasitic capacitance is analyzed in [14]. This method is based on the measured value of the parasitic capacitance, which depends on the position and spacing of the transformer wires. However, simply increasing the distance between the windings to reduce the parasitic capacitance can result in an increase in winding losses in terms of the current density because the window area cannot be utilized. In [15], several Litz-wire-based winding methods that reduced parasitic capacitance by minimizing the potential difference between windings were proposed. These winding methods use a thick Litz wire to reduce copper loss; however, these methods are difficult to implement in practice. In [16], it suggests minimizing the parasitic capacitance by increasing the section number of the transformer windings. more number of section and layer will gain smaller capacitance. but this method needs the fraction to divide windings and if there is too much section, then it is hard to get smaller capacitance. In [17], it analyzes how an outer fractional winding can impact the equivalent parallel capacitance of the magnetics and proposes a winding scheme that can reduce parallel capacitance. In [18], it analyzed the relationship between the number of layer and winding turns with the value of equivalent parallel capacitance and suggests the winding structure that has the lowest equivalent parallel capacitance. Not only parasitic capacitance, technique that reduces parasitic inductances by applying partial interleaving winding technique [19], [20] is also utilized in the transformer winding. But these methods only focus on the winding methods to reduce leakage inductance and it did not give tips about minimizing the parasitic capacitances. Therefore, an interleaved serpentine winding structure and a bobbin that achieves low parasitic capacitance without increasing the window area in a planar transformer are proposed in this paper. To verify the effectiveness of the proposed structure, the parasitic capacitance of the serpentine winding method and commonly used U-type winding method are analyzed theoretically, and an FEA simulation analysis is performed. The proposed winding method is employed to fabricate a 7.5 kW, 100 kHz high-frequency transformer prototype. The results of applying this prototype to the LLC resonant converter are presented and it is compared with the U-type winding transformer.

II. REVIEW OF THE WINDING METHOD APPLIED TO THE PLANAR TRANSFORMER

The advantages and disadvantages of the wire winding and PCB winding methods for manufacturing planar transformers are explained and the differences between the two methods are compared. Further, a suitable winding method for the high-density and high-efficiency planar transformer under high-current operating conditions is presented.

In the transformer design stage, design variables such as magnetizing inductance, current magnitude, and gain ratio are considered to determine the core, winding type, cross-sectional area, and number of turns [21]. The number of turns is increased to generate a high magnetizing inductance, and a winding with a thicker cross-section is selected to reduce the loss in the winding with a high operating current. Meanwhile, the core should have an appropriate cross-sectional area to ensure that the magnetic flux density does not exceed the limit value of the magnetic flux density. A core with a wider core window area is required in a transformer with high current input conditions and a large magnetizing inductance because it makes the winding thick, requires more turns, and consequently, increases the overall volume of the transformer. Therefore, the transformer window area should be used efficiently to achieve a high-power density. The height of the window space can be designed to be lower than that of a general core if a planar core is used to increase the power density of the converter. Thus, windings should be appropriately selected and arranged.

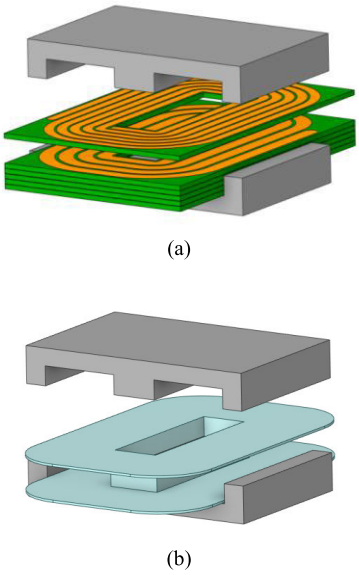

FIGURE 1. Structure of the transformer according to the winding method. (a) PCB winding method based transformer. (b) Wire winding method based transformer with a typical bobbin.

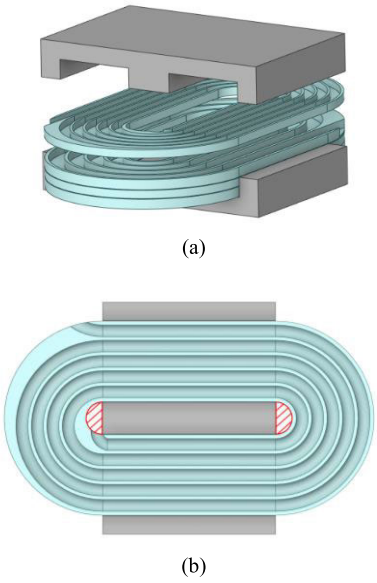

FIGURE 2. (a) Transformer with proposed stacked bobbin. (b) Top view of the stacked bobbin.

As shown in Fig. 1, planar transformers are used for windings in a low-window space. The PCB winding method is used in the form shown in Fig. 1(a), and the required number of turns is implemented using a PCB pattern. The transformer efficiency decreases because of winding loss when the current density of the PCB pattern is high. Therefore, a low current density is obtained by increasing the number of layers of the PCB or using several PCBs in parallel. The core and winding are combined by stacking thin-plate PCBs inside the core window and by alternately stacking the primary and secondary PCBs of the transformer. Interleaving between windings can be realized easily, and as a result, the AC loss can be reduced which leads to improvement of the overall efficiency [22]. This also provides an arrangement that minimizes the potential difference between the windings because PCB windings can easily implement complex winding structures, which reduces parasitic capacitance.

In the PCB winding method, an area that can be occupied by the copper winding is small because of the PCB insulation layer. The manufacturing cost is higher than that of the Litz wire-based winding. Owing to these disadvantages, the PCB winding method is not suitable as a transformer winding method for high-current design conditions. The Litz wire winding method is used in transformer with a normal height rather than low-profile transformers. And it can realize a wider conductor area within the window area than that using the PCB Winding method. This method is suitable for high-current operating conditions and is used to wind the wire on the bobbin and encompass the top and bottom of the core, as shown in Fig. 1(b). The windings are wound from the center leg of the core, and the windings on the opposite side are wrapped around the first winding. This winding has difficulty in realizing an interleaving structure compared to the method of arranging windings by stacking PCBs. In addition, the allowable radius for bending the winding is limited when a thick Litz wire is used to reduce the winding loss. This also reduces the degree of freedom in the winding arrangement. The arrangement of the windings can be changed easily by organizing the windings in parallel to reduce the diameter of a single winding; however, the length of each winding in parallel should be the same. If there is a difference in the length of each winding, the current flows unequally for each winding because of the imbalance of the winding resistance, and this causes a circulating current, which consequently causes winding loss. In summary, the PCB winding method can be used to implement a complex winding structure using multiple PCBs through pattern design, and it has the advantages of easy interleaving and excellent assembly. However, it is not suitable for high-current operations because of its low window utilization. Conversely, the Litz wire-based winding method has advantages of being relatively suitable for high-current and high-frequency operations, but it is difficult to implement a complex winding method because of the limited radius curvature of the winding. Losses caused by circulating current should also be considered when windings are arranged in parallel. Therefore, for manufacturing a planar transformer with a high input current, the current density can be reduced using a Litz wire and the winding form should be adjusted for the interleaving structure. Thus, in this manner, the advantages of both the PCB winding and wire winding methods can be applied to the transformer.

III. PROPOSED INTERLEAVED SERPENTINE WINDING METHOD

An interleaved serpentine winding method using a Litz wire is proposed. This method has advantages of the PCB winding method, which is easy to implement in an interleaved

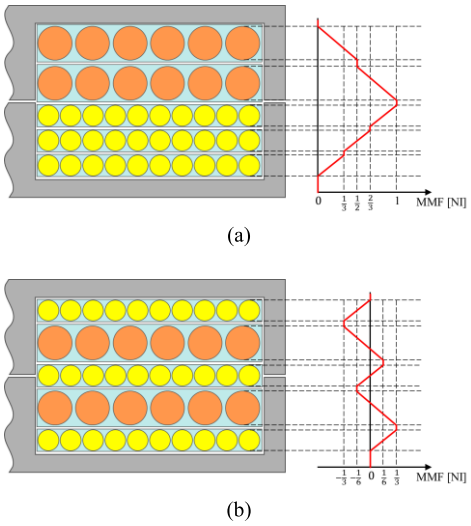

FIGURE 3. MMF (Magneto Motive Force) distributions. (a) Non interleaving arrangement. (b) Interleaving arrangement.

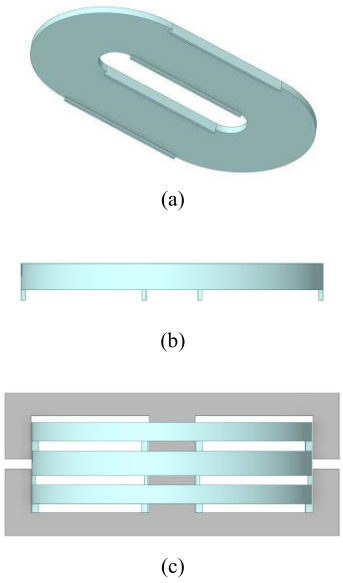

FIGURE 4. (a) Structure for constructing an air layer between stacked bobbins. (b) Side view. (c) Example of bobbins combined with cores.

structure arrangement and enables the balanced distribution of copper loss in parallel winding through a certain shape of multiple boards. The proposed winding method is shown in Fig. 2. The Litz wire is wound in the horizontal direction on the thin and flat bobbins shown in Fig. 2 to form a transformer with a flat core. The bobbin enables windings configured in parallel for the same length and shape. Further, the windings can be easily assembled and interleaved because a transformer is formed by stacking primary and secondary bobbins in the same way as in the PCB winding method. In addition, to reduce the parasitic capacitance of the planar transformer, the serpentine winding method, which arranges the windings alternately in the horizontal and vertical directions, is applied to minimize the potential difference between adjacent windings. This reduces the capacitive energy stored in the parasitic capacitance. The main contribution of this paper is to describe an effective bobbin structure and a winding technique using Litz wire for implementing serpentine winding in the transformer. While the technique of winding in a serpentine pattern using a PCB or coil that allows flexible shape adjustment has been explored in previous research, it is mostly applied in cases of transformers used under high current conditions, where winding with Litz wire-based techniques can offer advantages in terms of volume, losses, and thermal aspects compared to using PCB and coil. When applying the Litz wire-based serpentine winding with the proposed bobbin structure suggested in this paper, it is possible to effectively wind the coils in a serpentine pattern, and by stacking the proposed bobbin structure in an interleaved manner, AC losses can be reduced. Therefore, the main contribution of this study can be summarized as explaining an effective bobbin structure for implementing Litz wire-based serpentine winding and describing the winding technique considering parasitic capacitance and AC losses through stacked bobbin structures.

A. STRUCTURAL CHARACTERISTICS OF STACKED WINDING SYSTEM FOR INTERLEAVING

The multilayer bobbin method is used for constructing transformer by alternately stacking bobbins on which primary and secondary windings are wound so that an interleaved structure can be formed easily. The proposed bobbin is illustrated in Fig. 2. As shown in Fig. 2(b), the winding space can be formed by a barrier between the windings on an elliptical base (An ellipse is selected to maximize the radius of the curvature of the winding wire). If the barrier is too thick, the space that can be occupied by the winding within the bobbin is reduced and the window utilization rate is also reduced; this can offset the advantage of the Litz wire. Thus, it is necessary to select the appropriate barrier thickness because the horizontal spiral structure in the bobbin has a winding inside the transformer, and it is necessary to provide space for the wire inside to be removed. The space shown in Fig. 2(b) allows for the inner wire to be removed from the transformer, and it is formed symmetrically on both sides of the core so that both the primary and secondary sides can have a corresponding space. Even when several bobbins are stacked, the lead lines must not overlap with each other. And the space area must be larger than the total cross-sectional area of the Litz wire. Fig. 3 shows the distribution of the magnetomotive force based on the arrangement of the stacked bobbins. Six and ten turns are wound on the primary- and secondary-side bobbins, respectively, and it is composed of two parallels on the primary side and three parallels on the secondary side. The magnitude of the magnetomotive force exerted by one bobbin is the product of the number of the magnetomotive force inside the transformer. However, through interleaving, this value can be reduced by dividing it by the number of bobbins in parallel. An appropriate diameter of the winding wire and number of parallel windings must be selected

considering the height of the core window to maximize the effect of the stacked bobbin. Further, the diameter of the winding wire should be selected by dividing the window width by the number of turns minus the thickness of the bulkhead to reduce the DC loss when maximizing the window area. The height of the bobbin is the sum of the diameter of the selected winding wire and thickness of the base. The base should also be sufficiently thin to increase the utilization ratio of the window. When the dimensions of the primary and secondary windings and height of the bobbin are determined, the number of parallel bobbins should be selected to ensure that the current densities on both sides are similar. Meanwhile, the total height of the bobbin should be close to the window height of the transformer, and the unallocated window area, which is smaller than the minimum thickness of the bobbin, should be divided and arranged between the bobbins to reduce the magnitude of the parasitic capacitance. When using conventional bobbins to manufacture transformers with existing wires, there are certain limitations. The spaces allocated for interleaving become smaller as they get closer to the core, resulting in non-uniform volume distribution. Another issue arises when connecting the windings in parallel, as there can be an imbalance in copper losses, leading to circulating currents. On the other hand, connecting the windings in series and employing a sandwich structure, where the windings are alternately wound around the core, introduces challenges and increases the required time for the work, particularly when dealing with the intersection between the primary and secondary windings. To implement interleaving structure within the core window area, parallel divided windings are stacked horizontally, ensuring equal volume and shape for the divided space. This approach simplifies the fabrication process since windings on the same side share the same shape. To maintain a consistent winding shape, a bobbin with suitable grooves is utilized, aiding in the winding process. When stacking the bobbins, a slot is present to accommodate the wire drawn from the core's center to the outside. If a large number of turns are required during transformer design, the winding can be divided into two layers when employing a stacked bobbin. Unlike conventional transformers, the use of a multilayer bobbin enables the formation of flow spaces within the transformer's winding. A bobbin structure facilitating the creation of gaps between bobbins is shown in Figure 5. These air layers maximize the cooling effect of air-cooled heat dissipation through the use of a fan, and the low permittivity of the air gap reduces the parasitic capacitance. The interleaved structure achieved by winding and stacking the transformer wires horizontally for both primary and secondary windings simplify manufacturing processes. The horizontal winding method also creates air gaps between the stacked wires, facilitating airflow and making it an effective air-cooled heat dissipation method, especially when using a fan. This arrangement enhances heat dissipation and reduces parasitic capacitance. In addition to the effect of parasitic capacitance, heat management is also important. The temperature of the transformer increases because of the heat generated by the core and winding loss. Effective heat dissipation under high-current operating conditions can be achieved using this structure, as shown in Fig. 4. Fig. 4(a) shows that an air layer is formed between the stacked bobbins, which shows that structural protrusions exist under the bobbins. Fig. 4(b) shows that protrusions inside and outside the core window separate adjacent bobbins and simultaneously form a space for heat dissipation. The space makes air circulation more effective. If the fan is provided, it can more effectively improve the effect of heat dissipation and reduce the parasitic capacitance by disposing an air layer that generates relatively low permittivity between the bobbins.

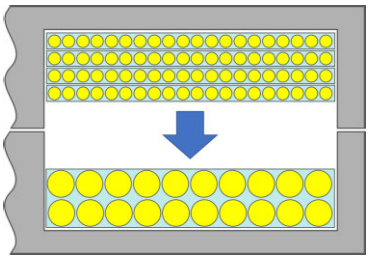

FIGURE 5. Comparison of single-layer structure and two-layer structure in 20 turns windings.

B. APPLICATION OF SERPENTINE WINDING METHOD TO STACKED BOBBIN

The winding diameter of the proposed laminated bobbin is the length divided by the window width, which can be calculated by considering the number of turns. Therefore, the winding diameter becomes extremely small when the number of turns is too large. A smaller winding diameter lowers the bobbin height and increases the number of bobbins required to fill the window height, and this increases the area occupied by the bobbin within the window area and reduces window utilization. In this case, a bobbin in the form of a two-layer structure is more effective than a single-layer structure. Fig. 5 shows the arrangement change when a single-layer structure is implemented as a two-layer structure. The structure increases the radius of the winding by halving the number of turns wound on one layer, which is equivalent to stacking four single-layer bobbins. Thus, a larger winding cross-sectional area can be allocated within the window area. However, this forms parasitic capacitance between layers within the bobbin, and thus, it has a limitation in that it cannot fundamentally solve the problem of parasitic capacitance [9]. Therefore, a layered bobbin-based serpentine winding method that can reduce the effect of parasitic capacitance is proposed. This method can minimize the potential difference between the windings without sacrificing the window area and power density of the transformer. Fig. 6 shows the potential distribution by layer and the potential difference between the layers of the U-type and Z-type winding methods, which are widely used among the existing winding methods and the proposed serpentine winding method proposed in this paper.

By comparing the proposed method with U-type and Z-type winding methods, the specific difference in the

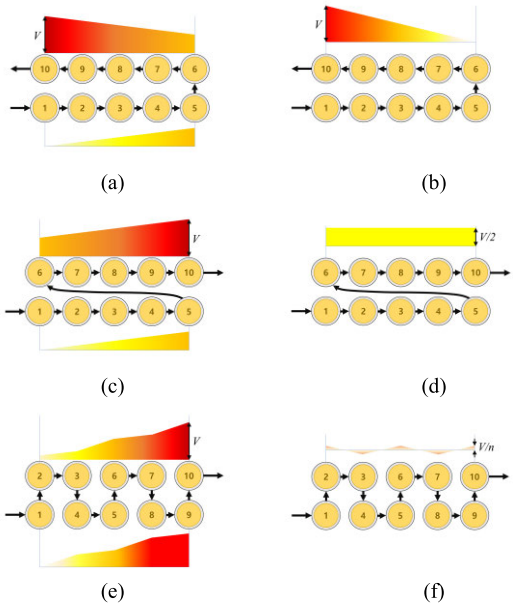

FIGURE 6. Potential distribution according to the winding method of a two-layer structure. (a) Potential distribution of the U-type winding method. (b) Potential difference between layers of the U-type winding method. (c) Potential distribution of the Z-type winding method. (d) Potential difference between layers of the Z-type winding method. (e) Potential distribution of the proposed serpentine winding method. (f) Potential difference between layers of the serpentine winding method.

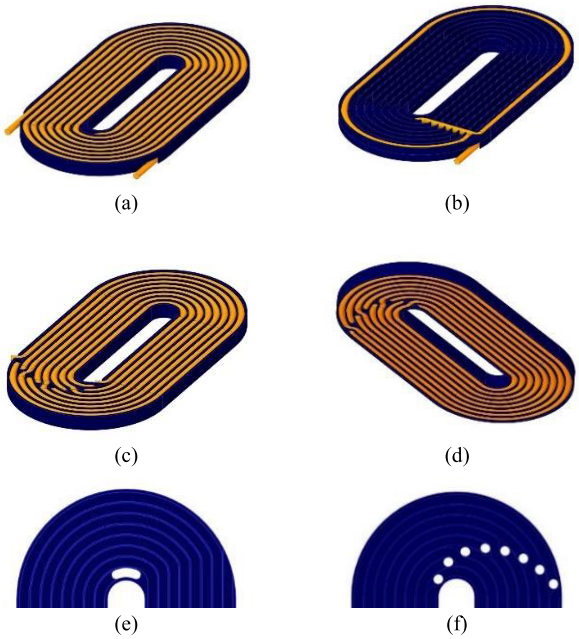

FIGURE 7. 3D model of the two-layer stacked bobbin. (a) Bobbin and winding of U-type winding method. (b) Winding arrangement for Z-type winding. (c) Bobbin and winding of serpentine winding method. (d) Lower side of serpentine winding. (e) Groove arrangement for U-type winding. (f) Groove and holes arrangement for serpentine winding.

winding method can be seen, and through this, the principle of reducing the magnitude of the parasitic capacitance in terms of voltage magnitude can be confirmed. In the U-type- and Z-type winding methods, all windings are wound in one layer and then carried over to the next layer. The potential difference between the layers is large at the end of the winding because the potential of the winding starting from the next layer is half the potential V across the transformer. The potential difference between the two layers is stored as capacitive energy in the parasitic capacitance, and the larger this energy, the larger is the effective value of the parasitic capacitance [22]. The potential differences between the layers for the two winding methods are shown in Figs. 6(b) and (d). The serpentine winding method has a horizontal spiral structure that alternately carries over the upper and lower layers in a two-layer structure. To apply the winding method to the laminated bobbin, the wire is carried vertically through the upper and lower layers. The potential distribution for each layer of the serpentine winding method and the potential difference between layers are shown in Figs. 6(e) and (f), respectively. The potential difference between layers is obtained by dividing the potential V applied across the transformer by the number of turns. Therefore, the capacitive energy of the parasitic capacitance can be effectively reduced, which can minimize the effective parasitic capacitance. Fig. 7 shows the 3D model implementation of a two-layer laminated bobbin for applying each winding method. The U-type winding method is a horizontal spiral structure that requires one carry-over groove to wind all layers and move to the next layer. We then move to the next layer through the carry-over groove and fill the bobbin with a horizontal spiral structure in the same manner. The completed bobbin is illustrated in Fig. 7(a), and the location of the carry-over groove is shown in Fig. 7(e). The Z-type winding method has a horizontal spiral structure in the first layer, which is the same as the U-type winding method, but as shown in Fig. 7(b). The winding structure that crosses the bobbin after layer carry-over has a limitation in that it is difficult to realize a horizontal spiral structure. Thus, it is not suitable for laminated bobbins. The serpentine winding method applied to the laminated bobbin is shown in Figs. 7(c) and (d). Each figure shows the top and bottom of the laminated bobbin. By arranging the path for the layer carry-over groove and the horizontal spiral structure, as shown in Fig. 7(f), the winding method can be implemented without an additional area compared to that with the bobbin to which the U-type is applied.

IV. DERIVING THE PROPOSED INTERLEAVED SERPENTINE WINDING METHOD

A method for estimating the magnitude of the effective parasitic capacitance of the two-layer multilayer bobbin-based U-type winding method and serpentine winding method is proposed. The energy method, which is one of the methods for inferring capacitance through the total sum of electric field energy presented by the applied voltage, was used in previous studies [23], [24]. When the applied voltage across the winding is V and the flux density is D, the electric field energy We stored in the parasitic capacitance is given by the electric

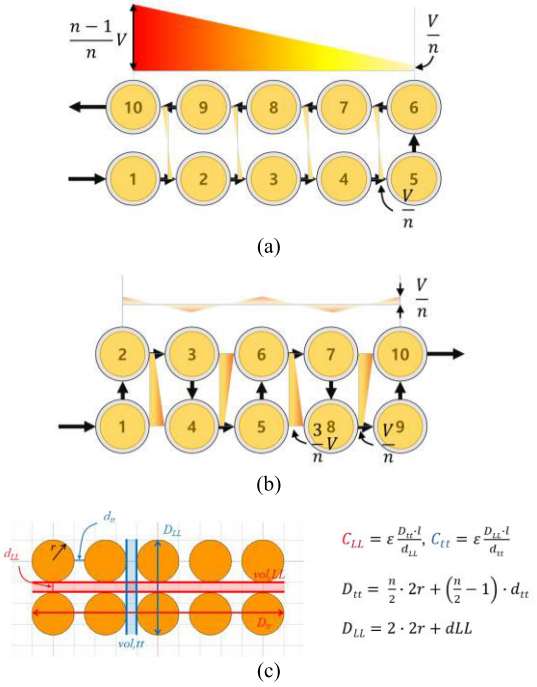

FIGURE 8. Layer-to-layer, turn-to-turn potential difference for the two-layer winding structure. (a) U-type winding method. (b) Serpentine winding method. (c) Parameters for calculating effective capacitance.

field energy is obtained by integrating the square value of the electric field strength E over space, and the parameter C_{eff} represents the effective capacitance for the applied voltage V. Figs. 8(a) and (b) show the potential differences between the layers and turns for the U-type and serpentine winding methods, respectively. These values should not be considered seriously when calculating the winding parasitic capacitance because the potential difference between the turns is considerably smaller than the potential difference between the layers [15].

$$W_e = \int_{vol} D \cdot E \, dv = \frac{1}{2} \int_{vol} \varepsilon \cdot E^2 \, dv = \frac{1}{2} C_{eff} \cdot V^2 \quad (1)$$

$$E(x) = \left(\frac{\left(\frac{n-2}{n} V\right) x}{D_{tt}} + \frac{V}{n} \right) / d_{LL}, \; E'(y) = \frac{V}{n} \cdot \frac{2y}{D_{LL}} / d_{tt} \quad (2)$$

However, in the serpentine winding method, the potential difference between turns is larger than the potential difference between layers, and therefore, these factors should be calculated. Both the electric field energy and electric field energy between turns are separately calculated in the x- and y-axes, respectively. For the U-type winding method, the accuracy of the formula is improved by considering the energy based on the potential difference between turns. As depicted in the Fig. 8(c), some parameters for distance between the windings for calculating the parasitic capacitance using the energy method is defined. Specifically, D_{tt} is the horizontal length of all windings and D_{LL} is the vertical length of all windings. And d_{tt} and d_{LL} are the length of horizontal and vertical length of each winding.

$$\begin{aligned} W_e &= W_{e,x} + W_{e,y} \\ &= \frac{1}{2} \int_{vol,LL} \varepsilon E(x)^2 \, dv_{LL} + \frac{1}{2} \int_{vol,tt} (n-2) \varepsilon E'(y)^2 \, dv_{tt} \\ &= \frac{1}{2} \cdot \frac{1}{3} \left(1 - \frac{1}{n} + \frac{1}{n^2}\right) \cdot \varepsilon \cdot \frac{D_{tt} \cdot l}{d_{LL}} \cdot V^2 \\ &\quad + \frac{1}{2} \cdot \frac{1}{3} \left(\frac{1}{2n} - \frac{1}{n^2}\right) \cdot \varepsilon \cdot \frac{D_{LL} \cdot l}{d_{tt}} \cdot V^2 \end{aligned} \quad (3)$$

$$C_{eff} = \frac{1}{3} \left(1 - \frac{1}{n} + \frac{1}{n^2}\right) C_{LL} + \frac{1}{3} \left(\frac{1}{2n} - \frac{1}{n^2}\right) C_{tt} \quad (4)$$

In order to derive the value of the electric field, the formula can be composed of number of turns, voltage, and the length parameters. The strength of the electric field when applying the energy method to the U-type winding method is provided by (2), which was derived by assuming that the potential increased constantly with distance. In E(x), x increased from 0 to d_{LL} in the direction of the turn, which indicates a potential change.

$$E'(x) = \left(\frac{\frac{V}{n} x}{\frac{D_{tt}}{n-2}} \right) / d_{LL}, \; E'(y) = \left(\frac{2y}{D_{LL}} + 1 \right) \cdot \frac{V}{n} / d_{tt} \quad (5)$$

$$\begin{aligned} W_e &= W_{e,x} + W_{e,y} \\ &= \frac{1}{2} \int_{vol,LL} (n-2) \varepsilon E'(x)^2 \, dv_{LL} \\ &\quad + \frac{1}{2} \int_{vol,tt} \left(\frac{n}{2} - 1\right) \varepsilon E'(y)^2 \, dv_{tt} \\ &= \frac{1}{2} \cdot \frac{1}{3n^2} \cdot \varepsilon \cdot \frac{D_{tt} \cdot l}{d_{LL}} \cdot V^2 \\ &\quad + \frac{1}{2} \cdot \frac{13}{3} \left(\frac{1}{2n} - \frac{1}{n^2}\right) \cdot \varepsilon \cdot \frac{D_{LL} \cdot l}{d_{tt}} \cdot V^2 \end{aligned} \quad (6)$$

$$C_{eff} = \frac{1}{3n^2} C_{LL} + \frac{13}{3} \left(\frac{1}{2n} - \frac{1}{n^2}\right) C_{tt} \quad (7)$$

In E′(y), y increases up to $D_{LL}/2$ because the potential difference is 0 at the midpoint of the layer, and it represents the potential change. Owing to the repeatability of the winding method, the electric field energy distribution was repeated identically. To simplify the calculation, the prime (′) symbol is used to indicate that the value is part of the entire electric field, and the redundancy can be determined by the number of turns. To obtain these results, the number of times should be multiplied to calculate the total energy. After substituting (2) into (1), the results can be derived as in (3). The domain integrated in the process of obtaining the energy between each turn is equal to the domain of E′(y). The effective capacitance calculated for the U-type winding method can be expressed using (4). In this equation, the formula for effective capacitance is composed of the number of turns and parameters for horizontal effective capacitance C_{tt} and vertical capacitance C_{LL}. The same process was repeated to derive the effective capacitance for the serpentine-winding method. Equation (5) represents the strength of the electric field when applying the energy method to the serpentine winding method. In (2), only a partial electric field strength is shown for the repeated

TABLE 1. Default setting value for simulation.

Parameter	Value	Unit	Parameter	Value	Unit
Total turns	10	Turn	Voltage between turns	100	V
Winding diameter	5.1	mm	Winding length	1 (unit)	m
Distance between layers	1	mm	Distance between turns	1	mm

TABLE 2. Correction factor for each winding method.

U-type winding method		Serpentine winding method	
Radius r correction factor	1.05	Radius r correction factor	1
d_{LL} correction factor	1.3	d_{LL} correction factor	0.15
d_{tt} correction factor	0.15	d_{tt} correction factor	0.9

structure, which rearranges the domain *vol* and multiplies it by the number of iterations to derive the total energy value in the integration process. Substituting (5) into (1), the equations for the final effective capacitance of the serpentine winding method are given by (6) and (7). To compare the parasitic capacitance of each winding method, subtract (7) from (4) and (8) can be derived.

$$C_{difference} = \frac{1}{3}\left(1 - \frac{1}{n}\right) C_{LL} - 2\left(\frac{1}{n} - \frac{2}{n^2}\right) C_{tt} \quad (8)$$

In (8), $C_{difference}$ means the parasitic capacitance difference between U-type winding and proposed one. if the value of C_{LL} is equal to C_{tt}, the value of (8) becomes positive when the number turns exceeds 4 turns. In general, the value C_{LL} is much bigger than C_{tt}. therefore, the difference between U-type and proposed winding method becomes also positive under the conditions that turns are less than 4 turns. the detailed analysis of (8) is included in the Appendix to verify the theoretical improvement effect of the proposed winding method.

V. RESEARCH VERIFICATION

A. VERIFICATION OF DERIVED FORMULA AND CORRECTION FACTOR SELECTION

The formula derived in Section IV was validated by comparing it with the results of the FEA program. The formula derived through the energy method assumes that the energy stored between the windings is the same as the capacitance of the parallel plate structure, and therefore, if the magnitude of the potential increases, errors between the formula and the actual result are inevitable. To reduce this error, a correction factor was added to each winding radius r, insulation distance d_{LL} between layers, and insulation distance D_{tt} between turns, which were selected when designing a flat bobbin. Simulations were conducted to verify the validity of the derived formulae, and Tables 1 and 2 list the default parameters for the FEA 2D analysis simulation and correction factors for

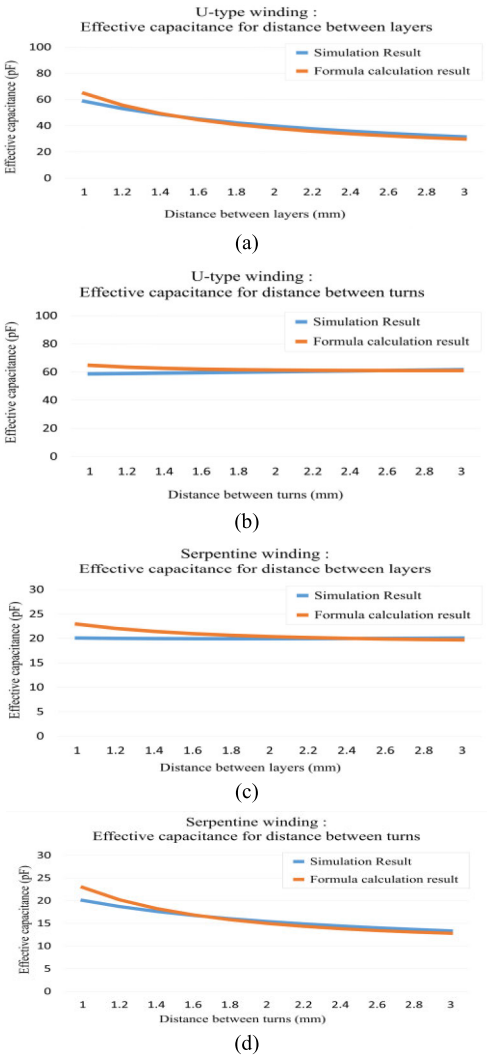

FIGURE 9. Comparison of effective capacitance of U-type and serpentine winding methods according to changes in the distance between layers and between turns, and a comparison of simulation and formula results.

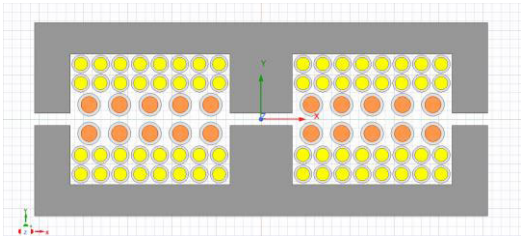

FIGURE 10. 2D FEA modeling of the proposed serpentine winding-based transformer.

each winding method, respectively. In the U-type winding method, there is a large potential difference between the layers and the stored energy, and therefore, the effect of the length d_{tt} between turns is insignificant. Thus, the correction coefficients of d_{tt} for the U-type winding method and d_{LL} for the serpentine winding method were selected as 0.15. For the values of the other correction coefficients, the value that

TABLE 3. Winding design parameter.

Primary winding parameters			Secondary winding parameters		
Total turns	5	Turn	Total turns	16	Turn
V_{peak}	237	V	V_{peak}	740	V
I_{RMS}	57.04	A	I_{RMS}	16.8	A
Winding diameter	5.1	mm	Winding diameter	4	mm
Cross - sectional area	10.2	sq	Cross-sectional area	6.8	sq
Number of parallel bobbins	2	-	Number of parallel bobbins	2	-

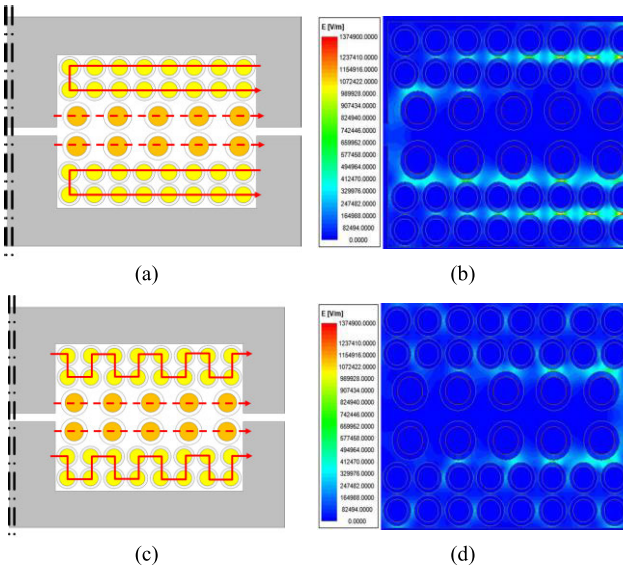

FIGURE 11. Comparison of capacitive energy distribution according to the winding method. (a) U-type winding method modeling. (b) Capacitive energy distribution for U-type winding method. (c) Serpentine winding method modeling. (d) Capacitive energy distribution for serpentine winding method.

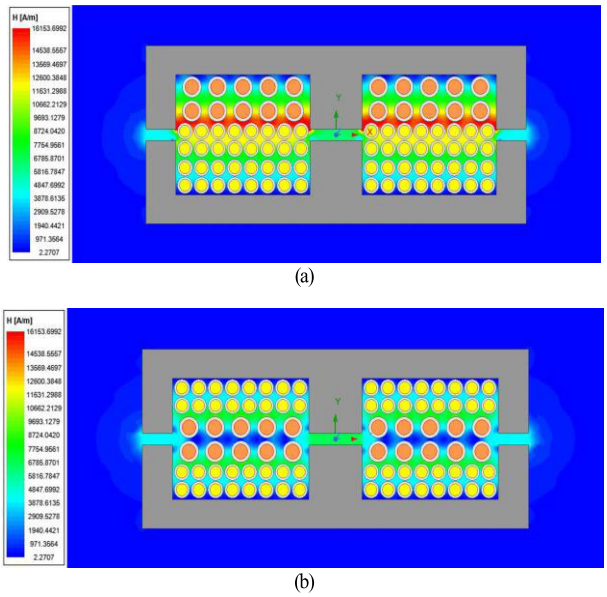

FIGURE 12. (a) Magnetomotive force distribution in noninterleaving arrangement of stacked bobbins. (b) Magnetomotive force distribution in the interleaving arrangement of stacked bobbins.

FIGURE 13. Planar transformer using the interleaved serpentine winding method.

TABLE 4. System parameter.

Parameter	Value	Unit	Parameter	Value	Unit
Input voltage	120-230	V_{DC}	Output voltage	400–600	V_{DC}
Nominal input voltage	237	V_{DC}	Nominal output voltage	500	V_{DC}
Output power	7.5	kW	Resonant frequency	100	kHz
Operating frequency	50–250	kHz	Magnetizing inductance	10.2	μH
Resonant capacitance	825	nF	Resonant inductance	2.75	μH

resulted in the smallest error was selected by comparing the calculated value with the FEA simulation result. The graphs in Fig. 9 show the equations and simulation results to which the correction coefficient was applied. The maximum error was less than 15%. Thus, the formula confirmed that the effective value of the parasitic capacitance of the serpentine winding method was smaller than that of the U-type winding method.

B. SIMULATION AND EXPERIMENTAL RESULTS

As shown in Fig. 10, the cross-section of the transformer is modeled in 2D and the electromagnetic field is analyzed using the analysis program to confirm the effect of reducing the parasitic capacitance and AC loss of the interleaved serpentine winding method. The modeled transformer has five turns on the primary side and 16 turns on the secondary side. It was designed under the operating condition of a primary-side peak voltage of 230 V and a secondary-side peak voltage of 740 V. Table 3 lists the additional design parameters for the windings. The primary side has a single-layer horizontal spiral structure, and the secondary side has a two-layer structure because of the large number of turns. Both the primary and secondary sides are composed of two parallel bobbins stacked in the order of S-P-P-S for interleaving, as shown in Figs. 11(a) and (c). The arrangement of the secondary side winding is configured with the U-type winding method

TABLE 5. Comparison between proposed and other transformer.

Other Transformer			Proposed Transformer		
PARAMETER	VALUE	UNIT	PARAMETER	VALUE	UNIT
L_m	10.26	uH	L_m	10.21	uH
L_{lkp}	0.54	uH	L_{lkp}	0.07	uH
L_{lks}	5.1	uH	L_{lks}	0.86	uH
T_{core}	Δ31.3	°C	T_{core}	Δ27.7	°C
$T_{winding}$	Δ47.3	°C	$T_{winding}$	Δ40.0	°C
efficiency	96.7	%	efficiency	97.2	%

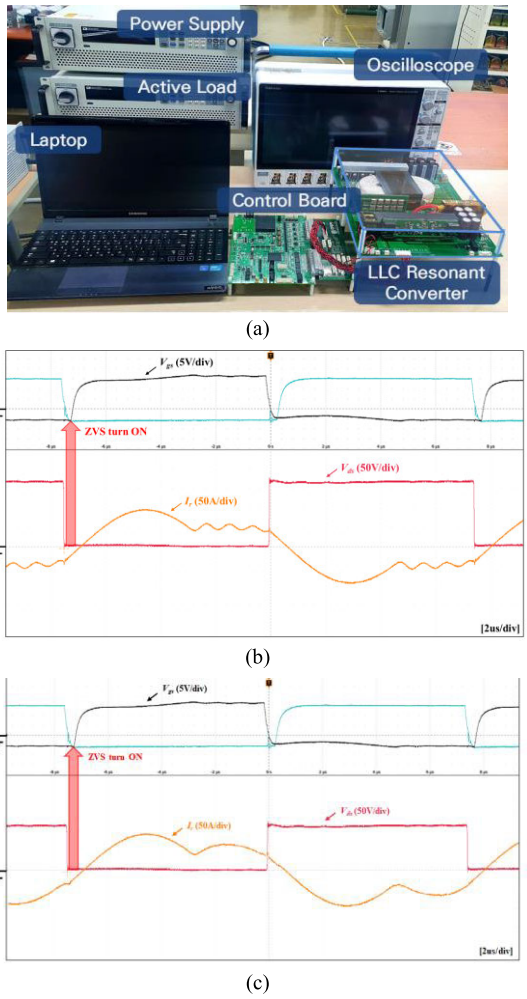

FIGURE 14. (a) Experimental setup for 7.5 kW LLC resonant converter with proposed planar transformer. (b) Experimental waveform without considering serpentine winding method. (c) Experimental waveform applying the proposed serpentine winding method.

and the serpentine winding method; the simulation is conducted as shown in Fig. 11. The simulation results shown in Fig. 11(b) and (d) confirm that the capacitive energy distribution of the serpentine winding method is smaller than that of the U-type winding method, which indicates a reduction in the effective value of the parasitic capacitance. To compare the intra-winding capacitance and inter-winding capacitance in Figure 11 (b) and Figure 11 (d), the energy magnitudes within winding regions were measured and compared using 2D Finite Element Method (FEM). In Figure 11 (b), it can be observed that when the U-type winding method is used, the average magnitude of intra-winding energy for the primary and secondary windings is measured at 1.81E+05 [V/m], and the average inter-winding energy is measured at 3.02E+05 [V/m]. On the other hand, when the proposed winding method is used, the average size of intra-winding energy is measured at 0.667E+06 [V/m], and the inter-winding energy is measured at 1.77E+05 [V/m]. It can be seen that the intra and inter-winding energies are relatively smaller when the proposed winding method is used compared to the U-type winding method. This relative comparison of inter and intra energy indicates that the inter and intra-winding capacitance in the proposed winding method would be smaller compared to the U-type winding method. To derive the specific value of inter-winding and intra-winding capacitance, the estimation of effective capacitance proposed in this paper was used for calculation of intra-winding capacitance, while the method described in [24] was employed for inter-winding capacitance. Through this, it can be determined that when the U-type winding method is applied, the estimation value of inter-winding capacitance is 27.67 [pF], and the value of intra-winding capacitance is 17.9 [pF]. In addition, to verify the effect of the interleaving of stacked bobbins shown in Fig. 12, the distribution of the magnetomotive force with or without the application of the interleaving structure is confirmed through FEA simulation. When the interleaving structure is applied to stacked bobbins configured in parallel, the maximum value of the magnetomotive force generated inside the transformer is reduced to half of that of the conventional size. Specifically, when the existing U-type winding method is applied, the maximum value of magnetic field intensity is 16153.7 [A/m]. However, when the proposed winding method is applied with interleaving technique, the maximum value of magnetic field intensity is 8232.4 [A/m]. The magnitude of leakage inductance increases as the MMF increases, indicating that the leakage inductance is significantly higher when the U-type winding method is applied. In practice, when the U-type winding method and the serpentine winding method were applied separately under the same conditions to produce a transformer magnetizing inductance to achieve the same value of 10.2 [uH], the U-type winding method resulted in a primary leakage inductance of 0.54 [uH] and a secondary leakage inductance of 5.1 [uH]. On the other hand, when the serpentine winding method was applied, the primary leakage inductance was measured at 0.07 [uH], and the secondary leakage inductance was measured at 0.86 [uH]. Through this, it can be observed that the proposed technique has the advantage of being able to design the leakage inductance much smaller compared to the existing U-type winding method. Finally, a planar transformer prototype with an interleaved serpentine winding method was manufactured, and an experiment was conducted to verify the effectiveness of the prototype. Fig. 13 shows the actual prototype of the transformer; the used core was ELP 102/20/38 from

EPCOS and material type is FM10, and material type of stacked bobbin is PA-CF high heat resistance filament and it is manufactured by using a 3D printer. The experimental environment is configured as shown in Fig. 13(a). It is an LLC resonant converter with a capacity of 7.5 kW, and the overall height of the converter is less than 45 mm when applying a planar transformer. To obtain a high gain ratio to satisfy the design requirement of voltage conversion from the lowest input voltage (120 V) to the maximum output voltage (600 V), the transformer operates in a frequency range lower than the resonance frequency and there is an interval in which the circulating current flows through the magnetizing inductance of the transformer. Meanwhile, ringing occurs because of the resonance of the parasitic capacitance and the inductance of the transformer. If these effects become dominant, then it can deteriorate the stable operation of the LLC converter. And also these effects make it difficult to derive an accurate voltage gain curve, which is necessary for designing an LLC resonant network system. However, when the proposed serpentine winding method is applied as shown in Fig. 14(c), the effect of parasitic capacitance decreases by observing the resonant current waveform. The ringing component included in the resonant current also decreases. Using the proposed winding method, the effect of parasitic capacitance reduction can be verified, and this improves adverse effects of parasitic capacitance that affects the resonant current during the circulating interval and helps to design the accurate resonant network without considerably take into account the parasitic effect of the capacitance. To be specific, the measured inductance, temperature, and efficiency for both the existing U-type winding-based transformer are summarized in Table 5. The designed magnetizing inductance value for both cases is 10.2 [uH], and the corresponding leakage inductance sizes are listed in the table. It can be observed that the magnitude of leakage inductance is larger for the existing winding method, indicating that the coupling coefficient is relatively larger for the proposed winding method. Furthermore, the proposed winding method results in a smaller MMF magnitude and hence lower AC losses compared to the existing method, indicating that the core and average temperatures for the primary and secondary windings are not significantly high compared to the existing U-type method. This suggests that the magnetics losses are also relatively small. Using this transformer, when driving a 7.5 kW LLC resonant converter under nominal conditions, the efficiency of the proposed winding-based converter is measured at 97.2%, while the efficiency of the existing winding method is 96.7%. This indicates an improvement of approximately 0.5% in efficiency compared to the existing method. Thus, the proposed winding method has been validated to be superior to the existing method not only in terms of parasitic capacitance within the transformer but also in terms of leakage inductance and efficiency. In terms of resonance frequency, the parameters of the resonant capacitor, inductor, and transformer were set to achieve a resonant frequency of 100 kHz in the initial design step. However, when implementing the existing winding method in the designed resonant network, the resonant frequency decreased to 96.9 kHz during experiment due to the impact of parasitic capacitance. In contrast, when employing the proposed winding method, the effect of parasitic capacitance can be reduced compared to the conventional winding method. As a result, a resonance frequency is 99.1 kHz which indicates an improvement in maintaining the desired resonant frequency compared to the existing winding method.

VI. CONCLUSION

A multilayer bobbin and low parasitic capacitance serpentine winding method for interleaving transformer windings were proposed. A Litz wire, which has the advantages of high-current and high-frequency operation, was wound on a multilayer bobbin to facilitate interleaving and minimize the potential difference between layers by applying the serpentine winding method in a two-layer multilayer bobbin structure for the required turns, and it makes low ac loss. To estimate the effective capacitance of the proposed structure and the existing winding method, an effective capacitance calculation formula was derived using the energy method. Further, the error between the formula and FEA simulation results became small by applying a correction factor. The distribution of the capacitive energy and magnetomotive force of the U-type and interleaved serpentine winding methods were compared through FEA simulations; and also the effectiveness of the proposed winding method was verified through actual experiments. By reducing the parasitic capacitance and AC loss, it helps to achieve more precise and efficient design of resonant converters.

APPENDIX

Expanding (8) yields equation (9), where the numerator of the (9) corresponds to (10). And (10) can be expressed as (11) through formula expansion.

$$C_{difference} = \frac{(n^2 - n)C_{LL} + (12 - 6n)C_{tt}}{3n^2} \tag{9}$$

$$C_{difference1} = (n^2 - n)C_{LL} + (12 - 6n)C_{tt} \tag{10}$$

For 4 or more turns, C_{LL} in (11) becomes positive. Then remaining terms correspond to (12) by applying the definition of C_{LL} and C_{tt}. Expanding the equation (12) becomes (13). When the number of turns is 4 or more, the inequality $w \geq 2d$ holds true, resulting in a positive magnitude for equation (13).

$$C_{difference1} = \frac{3}{4}n^2 C_{LL} - 6nC_{tt} + 12C_{tt} + (\frac{1}{4}n^2 - n)C_{LL} \tag{11}$$

$$\varepsilon l \left(\frac{3}{4}n^2 \cdot \frac{w}{d} - \frac{12nd}{w(n-2)} + \frac{24d}{w(n-2)}\right) \tag{12}$$

$$3n\varepsilon l \cdot \frac{\left(w^2 n(n-2) - 16d^2 + \frac{32d^2 l}{n}\right)}{4dw(n-2)} \tag{13}$$

Hence, through the analysis, it can be observed that the magnitude of the capacitance of U-type winding method is larger than that of the proposed winding method for 4 turns or more.

REFERENCES

[1] J. Zeng, G. Zhang, S. S. Yu, B. Zhang, and Y. Zhang, "LLC resonant converter topologies and industrial applications—A review," *Chin. J. Electr. Eng.*, vol. 6, no. 3, pp. 73–84, Sep. 2020.

[2] A. Kolli, A. Gaillard, A. De Bernardinis, O. Bethoux, D. Hissel, and Z. Khatir, "A review on DC/DC converter architectures for power fuel cell applications," *Energy Convers. Manag.*, vol. 105, pp. 716–730, Nov. 2015.

[3] V. Boscaino, R. Miceli, C. Buccella, C. Cecati, H. Latafat, and K. Razi, "Fuel cell power system with LLC resonant DC/DC converter," in *Proc. IEEE Int. Electric Vehicle Conf. (IEVC)*, Dec. 2014, pp. 1–6.

[4] Z. Ouyang and M. A. E. Andersen, "Overview of planar magnetic technology—Fundamental properties," *IEEE Trans. Power Electron.*, vol. 29, no. 9, pp. 4888–4900, Sep. 2014.

[5] C. Quinn, K. Rinne, T. O'Donnell, M. Duffy, and C. O. Mathuna, "A review of planar magnetic techniques and technologies," in *Proc. APEC. 16th Annu. IEEE Appl. Power Electron. Conf. Expo.*, Mar. 2001, pp. 1175–1183.

[6] M. A. Saket, N. Shafiei, M. Ordonez, M. Craciun, and C. Botting, "Low parasitics planar transformer for LLC resonant battery chargers," in *Proc. IEEE Appl. Power Electron. Conf. Expo. (APEC)*, Mar. 2016, pp. 854–858.

[7] S. Ann, W.-J. Son, J. H. Lee, J. Byun, and B. K. Lee, "Design of a SiC-based LLC resonant converter for on-board chargers considering parasitic capacitance of planar transformer," in *Proc. 23rd Int. Conf. Electr. Mach. Syst. (ICEMS)*, Nov. 2020, pp. 315–319.

[8] M. A. Saket, M. Ordonez, M. Craciun, and C. Botting, "Common-mode noise elimination in planar transformers for LLC resonant converters," in *Proc. IEEE Energy Convers. Congr. Expo. (ECCE)*, Sep. 2018, pp. 6607–6612.

[9] M. A. Saket, N. Shafiei, and M. Ordonez, "LLC converters with planar transformers: Issues and mitigation," *IEEE Trans. Power Electron.*, vol. 32, no. 6, pp. 4524–4542, Jun. 2017.

[10] W. Chen, Y. Yan, Y. Hu, and Q. Lu, "Model and design of PCB parallel winding for planar transformer," *IEEE Trans. Magn.*, vol. 39, no. 5, pp. 3202–3204, Sep. 2003.

[11] Z. Ouyang, O. C. Thomsen, and M. A. E. Andersen, "The analysis and comparison of leakage inductance in different winding arrangements for planar transformer," in *Proc. Int. Conf. Power Electron. Drive Syst. (PEDS)*, Nov. 2009, pp. 1143–1148.

[12] Z. Ouyang, O. C. Thomsen, and M. A. E. Andersen, "Optimal design and tradeoff analysis of planar transformer in high-power DC–DC converters," *IEEE Trans. Ind. Electron.*, vol. 59, no. 7, pp. 2800–2810, Jul. 2012.

[13] C. Ropoteanu, P. Svasta, and C. Ionescu, "A study of losses in planar transformers with different layer structure," in *Proc. IEEE 23rd Int. Symp. Design Technol. Electron. Packag. (SIITME)*, Oct. 2017, pp. 255–258.

[14] S. E. Saravi, A. Tahani, F. Zare, and R. A. Kordkheili, "The effect of different winding techniques on the stray capacitances of high frequency transformers used in flyback converters," in *Proc. IEEE 2nd Int. Power Energy Conf.*, Dec. 2008, pp. 1475–1478.

[15] P. Thummala, H. Schneider, Z. Zhang, and M. A. E. Andersen, "Investigation of transformer winding architectures for high-voltage (2.5 kV) capacitor charging and discharging applications," *IEEE Trans. Power Electron.*, vol. 31, no. 8, pp. 5786–5796, Aug. 2016.

[16] L. Deng, P. Wang, X. Li, H. Xiao, and T. Peng, "Investigation on the parasitic capacitance of high frequency and high voltage transformers of multi-section windings," *IEEE Access*, vol. 8, pp. 14065–14073, 2020.

[17] B. Liu, R. Ren, F. Wang, D. Costinett, and Z. Zhang, "Winding scheme with fractional layer for differential-mode toroidal inductor," *IEEE Trans. Ind. Electron.*, vol. 67, no. 2, pp. 1592–1604, Feb. 2020.

[18] A. Massarini and M. K. Kazimierczuk, "Self-capacitance of inductors," *IEEE Trans. Power Electron.*, vol. 12, no. 4, pp. 671–676, Jul. 1997.

[19] M. Pavlovsky, S. W. H. de Haan, and J. A. Ferreira, "Partial interleaving: A method to reduce high frequency losses and to tune the leakage inductance in high current, high frequency transformer foil windings," in *Proc. IEEE 36th Power Electron. Specialists Conf.*, Jun. 2005, pp. 1540–1547.

[20] B. Chen, "Analysis of effect of winding interleaving on leakage inductance and winding loss of high frequency transformers," *J. Electr. Eng. Technol.*, vol. 14, pp. 1211–1221, May 2019.

[21] P. Sastinsky and M. Jendruch, "Design optimization of the power transformer and inductor in the switch-mode power supplies," in *Proc. 19th Int. Conf. Radioelektronika*, Apr. 2009, pp. 65–68.

[22] L. Dalessandro, F. D. S. Cavalcante, and J. W. Kolar, "Self-capacitance of high-voltage transformers," *IEEE Trans. Power Electron.*, vol. 22, no. 5, pp. 2081–2092, Sep. 2007.

[23] S. Kaboli and R. Farajidavar, "Improvement of the energy method for stray capacitance modelling of transformer winding in high voltage power supplies," in *Proc. IEEE 19th Workshop Control Model. Power Electron. (COMPEL)*, Jun. 2018, pp. 1–6.

[24] C. Østergaard, C. S. Kjeldsen, and M. Nymand, "Calculation of planar transformer capacitance based on the applied terminal voltages," in *Proc. IEEE 21st Workshop Control Model. Power Electron. (COMPEL)*, Nov. 2020, pp. 1–7.

SU-SEONG PARK received the B.S. degree in electrical engineering from Hanyang University, Seoul, South Korea, in 2020, where he is currently pursuing the Ph.D. degree with the Energy Power Electronics Control System Laboratory. His research interests include the design of high-density, high-efficiency power converters, the control of distributed power converter systems, renewable energy, and grid-connected inverter and microgrids.

MYEONG-SEOK JEON received the B.S. degree in electronic engineering from Hanyang University, Ansan-si, South Korea, in 2021, and the M.S. degree in electrical engineering from Hanyang University, Seoul, South Korea, in 2023.

His research interests include control technology for electric machines and power conversion circuits.

SUNG-SOO MIN received the B.S. degree in electrical engineering from Hanyang University, Seoul, South Korea, in 2019, where he is currently pursuing the Ph.D. degree with the Energy Power Electronics Control System Laboratory. His research interests include the protection and application of wide-bandgap devices and the design of high-density, and high-efficiency power converters.

RAE-YOUNG KIM (Senior Member, IEEE) received the B.S. and M.S. degrees in electrical engineering from Hanyang University, Seoul, South Korea, in 1997 and 1999, respectively, and the Ph.D. degree from the Virginia Polytechnic Institute and State University, Blacksburg, VA, USA, in 2009.

From 1999 to 2004, he was a Senior Researcher with the Hyosung Heavy Industry Research and Development Center, Seoul. In 2009, he was a Postdoctoral Researcher with National Semiconductor Corporation, Santa Clara, CA, USA, involved in a smart home energy management system. In 2016, he was a Visiting Scholar with the Center for Power Electronics Systems (CPES), Virginia Polytechnic Institute and State University. Since 2010, he has been with Hanyang University, where he is currently a Professor with the Department of Electrical and Biomedical Engineering. His research interests include the design of high-power density converters and the distributed control of power converters for modular power converter systems in applications of renewable energy, wireless power transfer, microgrids, and motor drives.

Dr. Kim was a recipient of the 2007 First Prize Paper Award from IEEE IAS.